Journal of Sol-Gel Science and Technology

Sol-gel synthesis of SrZr0.9Y0.1O 3-δ thin films for protonic ceramic electrolyser membranes

--Manuscript Draft--

Manuscript Number:	JSST-D-19-00791
Full Title:	Sol-gel synthesis of SrZr0.9Y0.1O 3-δ thin films for protonic ceramic electrolyser membranes
Article Type:	S.I. : 2019 XX Sol-Gel meeting St. Petersburg, Invited contributions
Keywords:	sol-gel; strontium zirconate; proton conductor; Protonic Ceramic Electrolyser; thin-film
Corresponding Author:	Jadra Mosa, PhD Institute of Ceramic and Glasses (ICV_CSIC) Madrid, SPAIN
Corresponding Author Secondary Information:	
Corresponding Author's Institution:	Institute of Ceramic and Glasses (ICV_CSIC)
Corresponding Author's Secondary Institution:	
First Author:	Ángel Triviño-Peláez
First Author Secondary Information:	
Order of Authors:	Ángel Triviño-Peláez
	Domingo Pérez-Coll, PhD
	Glenn Cristopher Mather, PhD
	Mario Aparicio, PhD
	Jadra Mosa, PhD
Order of Authors Secondary Information:	
Funding Information:	Ministerio de Ciencia, Innovación y Universidades (FPI BES-2016-077023) — Mr Ángel Triviño-Peláez
	Ministerio de Ciencia, Innovación y Universidades (ENE2015-66183-R) — Dr Glenn Cristopher Mather
	Ministerio de Ciencia, Innovación y Universidades (MAT2017-90695-3295-REDT) — Dr Glenn Cristopher Mather
	Ministerio de Ciencia, Innovación y Universidades (RTI2018-095088-B-I00) — Dr Glenn Cristopher Mather
Abstract:	Synthesis of the proton-conducting electrolyte SrZr0.9Y0.1O3-d (SZY) was undertaken by the sol-gel method employing an all-alkoxide route from reaction of strontium alkoxide produced in-situ and commercial zirconium and yttrium alkoxides. The solution was homogenized by a previous ligand exchange in 2-methoxyethanol to control the polycondensation rate and achieve SZY at the low final firing temperature of 700-800 °C. SZY thin films (~ 270 nm) were prepared by dip-coating on different substrates and characterised by scanning and transmission electron microscopy, grazing X-ray diffraction and confocal micro-Raman spectroscopy, revealing well crystallized SZY phase with orthorhombic symmetry (space group, Pnma). Impedance spectroscopy of a thin film deposited on a quartz substrate revealed that protons contribute to transport in wet conditions as confirmed by a lower conductivity in D2O-humidified air (1.02 eV) compared to H2O-wetted air (0.99 eV), with the difference in activation energy consistent with a conductive isotope effect.

Section/Category:	Sol-gel and hybrid materials for energy, environment and building applications
Additional Information:	
Question	**Response**

Graphical Abstract

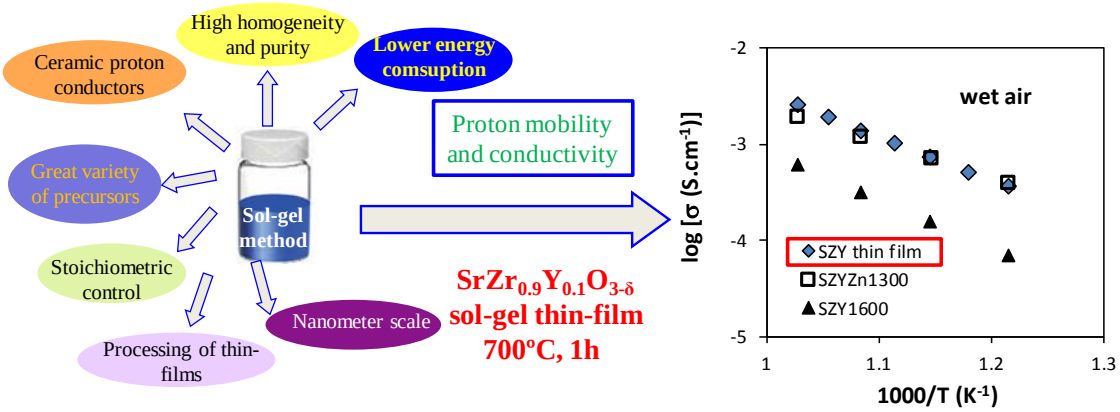

Proton-conducting electrolyte $SrZr_{0.9}Y_{0.1}O_{3-\delta}$ was synthesized by an all-alkoxide sol-gel method *via* initial *in-situ* formation of strontium alkoxide. SZY thin-film was well crystallized with orthorhombic symmetry at only 700 ºC, presenting conductivity similar to ceramic material assisted by Zn-sintering additive and sintered at high temperature.

Sol-gel synthesis of $SrZr_{0.9}Y_{0.1}O_{3-\delta}$ thin films for protonic ceramic electrolyser membranes

Ángel Triviño-Peláez, Domingo Pérez-Coll, Glenn C. Mather, Mario Aparicio, Jadra Mosa

Instituto de Cerámica y Vidrio (CSIC), Campus de Cantoblanco, 28049 Madrid, Spain

Abstract

Synthesis of the proton-conducting electrolyte $SrZr_{0.9}Y_{0.1}O_{3-\delta}$ (SZY) was undertaken by the sol-gel method employing an all-alkoxide route from reaction of strontium alkoxide produced *in-situ* and commercial zirconium and yttrium alkoxides. The solution was homogenized by a previous ligand exchange in 2-methoxyethanol to control the polycondensation rate and achieve SZY at the low final firing temperature of 700-800 °C. SZY thin films (~ 270 nm) were prepared by dip-coating on different substrates and characterised by scanning and transmission electron microscopy, grazing X-ray diffraction and confocal micro-Raman spectroscopy, revealing well crystallized SZY phase with orthorhombic symmetry (space group, Pnma). Impedance spectroscopy of a thin film deposited on a quartz substrate revealed that protons contribute to transport in wet conditions as confirmed by a lower conductivity in D_2O-humidified air (1.02 eV) compared to H_2O-wetted air (0.99 eV), with the difference in activation energy consistent with a conductive isotope effect.

Keywords: sol-gel; strontium zirconate; proton conductor; Protonic Ceramic Electrolyser; thin-film

1. Introduction

Hydrogen is currently an essential resource for many industrial processes, and may assume a key role as an energy vector in a future hydrogen economy [1,2]. Sustainable and environmentally benign ways of producing hydrogen are required to replace the principal current method dependent on reforming of fossil fuels. Electrolysis of steam employing a ceramic membrane is advantageous in this regard due to the greater thermodynamic efficiency at higher working temperature (500-1000 °C) in comparison to low-temperature electrolysis [3]. The use of waste heat from carbon-free methods of energy conversion, such as geothermal or nuclear, can further improve efficiency [4]. Protonic ceramic electrolysis cells (PCECs) are most promising for electrolysis since the possibility of working at a lower operation temperatures (<750 °C) in comparison to the oxide-ion-conducting ceramic cells (solid oxide electrolysis cells, SOECs) is favorable for long-term stability. Moreover, pure, dry hydrogen is produced in PCECs, eschewing the need for an additional drying step.

Strontium-zirconate-based perovskites, such as $SrZr(Y)O_{3-\delta}$ (SZY), are regarded as good candidates for the electrolyte material of PCECs due to their high mechanical and chemical stability [5,6]. Nevertheless, they are rather refractory with higher resistances than less-stable, proton-conducting perovskite families. Dense ceramic membranes are typically prepared by solid-state reaction, requiring high temperatures, ~ 1600 °C for SZY [7], to achieve the levels of gas impermeability required for electrolyte applications. This type of processing promotes large grain sizes which may be detrimental to mechanical strength and inhomogeneities are often present, which are difficult to remove from the final composition.

Alternative low-temperature, soft-chemistry methods can avoid some of the disadvantages of high-temperature processing. The sol-gel process permits a tighter control of the chemical composition of the material, softer heat treatments (temperature and time) and the possibility of controlled preparation of nanoparticles [8-10]. Another interesting advantage of the sol-gel method is the ability to prepare thin layers for electrochemical devices, which is especially relevant for reducing the Ohmic drop of the SZY electrolyte during electrolyser operation [11].

The typical approach for the preparation of complex materials, such as $SrZr_{0.9}Y_{0.1}O_{3-\delta}$, by sol-gel is usually based on the combination of alkoxide precursors and the metal salts. However, the different hydrolysis and condensation reactions rates may lead to inhomogeneities in the distribution of atoms and, consequently, the presence of secondary phases. In this context, sol-gel methods using only alkoxide precursors are very interesting for control over purity, chemical homogeneity and nanostructural uniformity. Nevertheless, the alkoxide mixture may still present complications due to the different hydrolysis rates of the precursors; hence the benefits of improved homogeneity can be lost during hydrolysis leading to mixed phases or non-ideal stoichiometry [12].

The objective in the present case is the synthesis of a mixed alkoxide with the three SZY cations before inducing polycondensation reactions that lead to gelation and the consolidation of the material after the appropriate heat treatment. Such a complex alkoxide precursor has the potential to result in a better control of stoichiometry at the molecular level, making it less sensitive to processing conditions. On the other hand, the formation of a thermodynamically ideal hetero-metal alkoxide assembly is dependent on various factors such as cation size and steric bulk of the alkoxo ligands. Hence, the synthesis of a hetero-metal precursor with a targeted ratio of metallic elements cannot

be achieved by simple mixing of the components in the required molar ratios. It first requires a strict control of processing conditions (solvents, complexing agents, pH, etc.) to produce a suitable heterometal alkoxide for the subsequent preparation of the multi-component metal oxide [9].

To the best of our knowledge, the literature does not report the synthesis of Sr-Zr-Y oxides by the sol-gel method, even combining salts and alkoxide precursors of the metals. Nevertheless, there have been some reports of employment of sol-gel for the synthesis of related compositions, such as $BaZr_{0.8}Y_{0.2}O_{3-\delta}$, using alkoxide precursors of the three metals [13]. Similar $BaZrO_3$-related compounds have also been prepared by combination of alkoxides [14-15]; however, a mixture of salts and alkoxides is mostly employed for such materials [16-18].

In this article, we report for the first time the sol–gel synthesis and coating on substrates of $SrZr_{0.9}Y_{0.1}O_{3-\delta}$ electrolytes for protonic ceramic electrolysers using a strontium alkoxide produced *in situ* which reacts with commercial zirconium and yttrium alkoxides. A key synthesis step is based on the use of 2-methoxyethanol as a ligand exchange that allows homogenization of the solution and control of the polycondensation rate to finally obtain a pure product using a soft thermal treatment. Thin films of SZY were deposited on quartz substrates, and preliminary determination of electrical properties of the films was undertaken employing impedance spectroscopy.

2. Experimental

$SrZr_{0.9}Y_{0.1}O_{3-\delta}$ coatings were prepared by the sol-gel method from a solution of purely alkoxide precursors developed using strontium (Aldrich, 99%), zirconium (IV) propoxide (Sigma-Aldrich, 70% in 1-propanol), and yttrium (III) butoxide (Aldrich, 0.5

M in toluene) as precursors. Strontium was dissolved in 2-methoxyethanol (ABCR, 98%) to produce a ligand exchange and obtain a homogeneous mix of alkoxides that leads to controlled condensation reactions, ensuring the preparation of homogeneous coatings [19]. All the chemicals were used without further purification. A glove box filled with argon was employed to weight the reagents and perform the synthesis of the precursor solution. Final molar ratios of strontium: zirconium (IV) propoxide: yttrium (III) butoxide: 2-methoxyethanol were 1.1:0.9:0.1:60. Strontium was added in excess to compensate a partial loss during the synthesis process and heat treatment of coatings. The zirconium (IV) propoxide and yttrium (III) butoxide solutions were mixed with 2-methoxyethanol and stirred at 70 °C for three hours in Ar atmosphere using a reflux system before cooling to room temperature. Subsequently, strontium was slowly incorporated by stirring at room temperature for one hour until dissolution; the sol was then stirred again at 70 °C for three hours. Coatings were prepared by dipping substrates in the alkoxide solution using a withdrawal rate of 26 cm min^{-1}. Three-layer coatings were prepared by repeating the dipping process after a drying step at room temperature for 30 minutes. A first thermal treatment at 150°C for two hours was performed in an argon atmosphere, and then treatments at 700, 800 and 900 °C for one hour in air were carried out to sinter the coatings and obtain the desired perovskite phase. Quartz substrates were used to assess the homogeneity and thickness of coatings and for electrochemical characterization; silicon substrates were employed for structural analysis.

Characterization of the coatings included analysis of a cross-section of coated samples performed by scanning electron microscopy (SEM) with a HITACHI S-4700 field-emission instrument. Spectral ellipsometric measurements were performed using a variable angle spectroscopic ellipsometer (WVASE32, M-2000UTM, J.A. Co.,

Woollam) to measure the thickness of the coatings deposited on quartz substrates. The crystal structure of the coated samples was characterized by grazing incidence X-ray diffraction using a Siemens D-5000 diffractometer. The crystallite size, ϕ, was calculated using the Scherrer's equation [20]:

$$\phi = \frac{0.94\,\lambda}{cos\theta\sqrt{B^2 - B_i^2}} \quad (1)$$

where θ is the angle of the diffraction maximum, B its full width at half maximum, B_i the instrumental broadening and λ is the wavelength. The θ and B parameters were obtained by fitting the peaks to pseudo-Voigt functions.

A JEOL TEM 2010 (200 kV) high resolution transmission electron microscope (HRTEM) with a point of resolution of 0.19 nm equipped with a Gatan CDD camera was used to both confirm the particle size of the crystalline phase in the coatings and characterize the crystal structure. Samples were prepared by scratching the coating followed by wet-grinding of the scratched material with absolute ethanol, then dropping the solution onto carbon-coated copper grids followed by drying under a UV lamp. A Raman study was carried out using a Confocal Micro-Raman (Witec alpha-300R) with laser excitation of 532 nm and a 100× objective lens (NA = 0.9) for coatings deposited on silicon substrates. The optical resolution diffraction of the Confocal Microscope is limited to 200 nm laterally and 500 nm vertically; Raman spectral resolution of the system is down to 0.02 cm^{-1}. The selected areas analyzed were 10 µm- 10 µm, acquisition time was 3.6 seconds for one single spectrum and the Raman image consists of 3000 spectra.

The electrical behaviour of a thin film of SZY on a quartz substrate treated at 700 °C was performed by in-plane impedance spectroscopy in a 2-probe configuration. Two

parallel, linear Pt electrodes were applied by painting Pt paste over the film at a distance of 4.7 mm and sintering the substrate-film assembly at 700 ºC for 1 hour. Four Pt wires were attached to the electrodes, with one pair yielding the current flow and the other the potential drop between the electrodes. Impedance spectroscopy was performed with an Autolab PGStat302N instrument operating in potentiostatic mode with a voltage amplitude of 50 mV in the frequency range $1 \leq f \leq 10^{6}$ Hz. Electrical data were collected in dry air on cooling in the temperature range 550-700 °C in steps of 25 °C.

3. Results and discussion

3.1 Sol-gel synthesis of SZY

We shall describe how a previous ligand exchange in 2-methoxyethanol is an important issue to homogenize the solution and control the polycondensation rate to finally obtain a pure product employing a very soft thermal treatment. The solution in the first step, after the incorporation of zirconium (IV) propoxide and yttrium (III) butoxide onto 2-methoxyethanol followed by stirring at 70 °C for three hours and then cooling to room temperature, is transparent and yellowish with a viscosity of 3.5 mPa s. Mixed organic solvents were subsequently added in the sequence i-propanol then n-butanol. Strontium filings were obtained inside the glovebox from drilling strontium dendritic pieces, weighed and added to the solution. The resulting solution was clear, brown and free of precipitates. The sol viscosity was ~ 2.0 mPa s at room temperature immediately after the synthesis, and did not change significantly in the following two weeks. Synthesis of triple-metal alkoxides containing strontium, yttrium and zirconium was achieved through alcohol exchange and condensation of metallic strontium, with zirconium and

yttrium alkoxide in a solution of alcohol and some organic solvent, resulting in the formation of a triple metal alkoxide and evolution of hydrogen gas [21]

$$M + ROH \rightarrow MOR + 1/2H_2\uparrow \quad (2)$$

A trimetallic precursor has the potential to control metal stoichiometry at the molecular level and thus make this critical parameter less sensitive to processing conditions, avoiding undesired second phases. The hydrolysis of heterometallic precursors, mixing alkoxides and salts with very different hydrolysis rates may result in metal precipitation [22-23]. Their advantage over inorganic salt mixtures, however, is that two or more elements of the final product are present, eliminating the need to match the reaction rates required from a multicomponent precursor mixture as required by conventional methods [11].

Triple metal alkoxides solutions as source precursors already contain metal-oxygen bonds. Because of this, thermal decomposition can be performed at relatively low temperatures while maintaining the the M-O core. It is extremely important to note that this method based on *in-situ* synthesis of triple alkoxide Sr^{2+}-Y^{3+}-Zr^{4+} can generate ceramic materials in a single step, resulting in high phase purity at low temperature, with specific properties such as high hardness, chemical and mechanical resistance, and high-temperature stability.

3.2 Structural analysis of SZY thin-films

Homogeneous and transparent coatings were obtained on both quartz and silicon substrates. Spectral ellipsometry measurements indicated a coating thickness of ~ 1.1 µm after drying at 150 °C. Coating thickness depends on the sol viscosity and specific

withdrawal rates used during the dipping process. The thickness decreases slightly with the increase of both the treatment temperature and sintering time, due to the elimination of solvents and organics, which slightly collapses the structure. The thickness of the coatings was approximately 1 μm for treatment at temperatures of 700 ºC, 800 ºC and 900 ºC, respectively.

Surface and cross-section scanning electron micrographs of the films deposited on a quartz substrate and heat treated at 700 and 800 °C for 1 hour are shown in Fig. 1. The surface image presents a homogeneous coating with nanoscaled grains (< 50 nm) at both temperatures, and the absence of precipitates or phase separations at this magnification. The image of the cross-section (Fig. 1c) reveals a well-bonded coating, in spite of the polishing process, with thickness ~ 1 μm, in agreement with the ellipsometry results.

Fig. 2 displays grazing incidence X-ray patterns of the sol-gel coatings treated at 700, 800 and 900 °C for one hour. The patterns are consistent with the orthorhombically distorted perovskite of SZY as the majority phase (JCPDS # 44-0161). On increasing the annealing time and temperature to 900 °C, the crystalline phase remains unchanged but precipitation of SrO (JCPDS # 48-1477) occurs, most probably resulting from the excess strontium used in the synthesis procedure. These are interesting results considering the soft thermal treatment conditions (temperature and time) in comparison with procedures based on solid-state reaction [7]. Analysis of the lattice constants of orthorhombically distorted $SrZr_{0.9}Y_{0.1}O_{3-\delta}$ perovskite phase (space group, *Pnma*) gave cell parameters of a = 5.81 Å, b= 8.18 Å and c= 5.79 Å, in good agreement with previously reported data for SZY [7].

The average crystallite size of the SZY phase was determined from the increasing broadening with decreasing temperature of the (002) XRD peak by the Debye Scherrer

formula. The crystallite size is ~ 18, 22 and 26 nm for final sintering temperatures of 700, 800 and 900 °C, respectively.

The HRTEM images of $SrZr_{0.9}Y_{0.1}O_{3-\delta}$ coating, synthesized by sol-gel and calcined at 800 ºC for 1 hour, are shown in Fig. 3. Small crystals are homogenously distributed along the coating. The results reveal the lattice planes and crystal-size distribution of SZY phase in the thin film. The crystal size is consistent with that obtained by XRD of ~ 22 nm at 800 ºC. Fourier transformation of the (002) crystal planes of the SZY phase was employed to estimate an interplanar distance of 0.29 nm (JCPDS 44-0161).

Since, generally speaking, secondary phases are often only present in trace amounts and may exhibit poor crystallinity due to their amorphous character, they are often difficult to detect using diffraction techniques alone. In contrast, the presence of traces of, among other species, carbonates, hydroxides and hydrates, gives rise to very characteristic peaks in Raman spectroscopy [24-26]. The Raman spectra of sol-gel coatings heat treated at different temperatures are shown in Fig. 4. The Raman spectrum of a perovskite compound can be considered as characteristic of a covalently bonded structure [6,27-28].

An ideal ABO_3 perovskite structure (space group $Pm\bar{3}m$, *Oh*) shows no Raman active modes, whereas the Raman spectra of the distorted $SrZr_{0.9}Y_{0.1}O_{3-\delta}$ perovskite structure present different active modes attributable to the orthorhombic symmetry [29-30]. The Raman spectrum (Fig. 4) confirms the orthorhombic symmetry of SZY as indicated by the characteristic triplet at 169, 148 and 115 cm^{-1} 31] and also reveals, for coatings heat-treated at 900 ºC, traces of impurities of SrO (narrow peak at 487 cm^{-1}) in agreement with the XRD results, Fig. 2 [32].

For all coatings, the spectra in the range < 200 cm^{-1} are characterised by vibrations of the Sr-ion network which couple with vibration modes of ZrO_6 iono-covalent entities leading to the lattice modes. The stretching and bending modes of the ZrO_6 octahedra are expected to lie in the ranges 600-900 cm^{-1} and 300-500 cm^{-1}, respectively. A broadening of the band in the 750-850 cm^{-1} region is observed in coatings heat treated at 800 and 900 ºC, which may be related to modification of the ZrO_6 octahedra by oxygen vacancies due to incorporation of Y^{3+} ions on the B sites [31]. Moreover, the bands located at 650 and 570 cm^{-1} decrease in intensity for coatings heat treated at 800 and 900 ºC, which could also be related to substitution of Zr ions by Y ions on the B sites, modifying the Zr-O and Sr-O stretching vibrations [33].

3.3 Electrical conductivity of SZY thin films

Typical impedance spectra of an SZY film on quartz substrate registered in wet air and D_2O-wetted air at 700 °C are shown in Fig. 5. The single semicircle in the impedance plane is fairly characteristic of thin films of ion-conducting materials measured on resistant substrates [34]. The very high values of geometrical factor (L/A), where L is the inner distance of the electrodes and A is the film cross-sectional area, leads to high resistance values and very low capacitances for the grain and grain-boundary components, as described previously [34]. The arc capacitance was estimated according to

$$C = Q^{1/n} R^{\frac{1-n}{n}} \quad (3)$$

where Q is the pseudo-capacitance related to the capacitance by the frequency power n. The calculated value corresponding to the arc in dry conditions in Fig. 5 of 2.52×10^{-12} F, much greater than that expected from the grain or grain-boundary components of the

film, is dominated by the stray capacitance of the substrate and equipment, reducing the system to a single RC element.

For wet oxidising conditions, mixed protonic-p-type electronic conductivities are expected in SZY [35]. Here, the observance of a conductive isotope effect, with lower conductivity registered in air humidified with D_2O in comparison to H_2O, indicates that this is indeed the case. The magnitude of the conductive isotope effect, determined by the ratio $\sigma(H_2O)/\sigma(D_2O)$ lies between 1.2-1.3, which is lower than that expected for a pure protonic conductor and may be associated to the contribution from the hole species in SZY, as was confirmed previously [35].

The Arrhenius behaviour of the electrical conductivity of the SZY thin film in wet air is represented in Fig. 6. The conductivity of the film is clearly higher than that obtained for the SZY pellet sintered at 1600 ºC, prepared in a manner described previously [7]. However, it lies close to the values obtained for an SZY pellet with 4 mol% ZnO sintered at 1300 ºC. The very low sintering temperature of the thin film may be responsible for the improvement of the specific grain-boundary conductivity, which would be reflected in the total electrical behaviour [7]. As mentioned, detailed analysis of transport numbers in SZY [35,36] indicates that in wet oxidising conditions, conductivity is dominated by mixed protonic and electron-hole transport. As a consequence, different preparation routes and sintering temperatures may have an inherent influence on the specific contributions of the various charge carriers (e.g. oxygen vacancies, protons and electron holes) with a different impact on the electrical conduction.

4. Conclusions

A mixed-alkoxide route was used for the low-temperature (700 °C) sol-gel synthesis of the proton-conducting electrolyte $SrZr_{0.9}Y_{0.1}O_{3-\delta}$, of interest for application in high-temperature electrolysis. A ligand exchange in 2-methoxyethanol is critical for homogenizing the solution and controlling the polycondensation rate to achieve the soft thermal treatment.

Thin films of SZY were deposited by dip-coating on quartz substrates and analysed by impedance spectroscopy. An H^+/D^+ isotope effect indicates that proton conductivity affects the electrical behaviour in humid atmospheres, although electron holes are also expected to be present.

Acknowledgements

We thank Ministerio de Ciencia, Innovación y Universidades of Spain for financial support (project ENE2015-66183-R, MAT2017-90695-3295-REDT, RTI2018-095088-B-I00 and student grant FPI BES-2016-077023). We also thank D. Ruiz and Dr. A. del Campo for their assistance with the experimental techniques.

Compliance with ethical standards

Conflict of interest The authors declare that they have no conflict of interest.

Publisher's note Springer Nature remains neutral with regard to jurisdictional claims in published maps and institutional affiliations.

References

1.Winter CJ (2005) Int. J. Hydrogen Energy 30:681-685.

2. Winter CJ, (2009) Int. J. Hydrogen Energy 34: S1-S52.

3. Ferrero D, Lanzini A, Santarelli M, Leone P (2013) Int. J. Hydrogen Energy 38: 3523-3536.

4. Petipas F, Brisse A, Bouallou C (2014) Int. J. Hydrogen Energy 39: 5505-5513.

5. Slodczyk A, Colomban P, André G, Zaafrani O, Grasset F, Lacroix O, Sala B (2012) Solid State Ionics 225: 214-218.

6. Slodczyk A, Zaafrani O, Sharp MD, Kilner JA, Dabrowski B, Lacroix O, Colomban P (2013) Membranes (Basel). 3:311-330.

7. Heras-Juaristi G, Pérez-Coll D, Mather GC (2016) J. Power Sources 331:435-444.

8. Hubert-Pfalzgraf LG, Daniele S, Decams J, Vaissermann M (1997) J. Sol-Gel Sci. Tech. 8(1-3):49-53.

9. Veith M, Mathur S, Mathur C (1998) Polyhedron 17 1005-1034.

10. Veith M, Mathur S, Lecerf N, Huch V, Decker T, Beck HP, Eiser W, Haberkorn R J. Sol-Gel Sci. Tech. (2000)17:145-158

11. Colomban P (2012) Sol-Gel Routes and Proton Conductors. In: Aparicio M, Jitianu A, Klein LC (eds) Sol-gel Processing for Conventional and Alternative Energy. Springer Science + Business Media Publishing, Basel, chapter 4.

12. Meyer F, Hempelmann R, Veith M (1999) J. Mater. Chem.9:1755-1763.

13. Cervera RB, Oyama Y, Yamaguchi S (2007) Solid State Ionics 178: 569-574.

14. Veith M (2002) J. Chem. Soc., Dalton Trans. 2405–2412.

15. Cervera RB, Oyama Y, Miyoshi S, Kobayashi K, Yagi T, Yamaguchi S (2008) Solid State Ionics 179: 236-242.

16. Hardy A, D'Haen J, Van den Rul H, Van Bael MK, Mullens J Mater. Res. Bull. (2009) 44:734-742.

17. Celik E., Akin Y, Mutlu IH, Sigmund W, Hascicek YS, (2002) Phys. C Supercond. Its Appl. 382:355-360.

18. Stenstrop G., Engell J., Less-Common Met J. (1990) 164165: 200-207.

19. B Su, KL Choy (1999) J. Mater. Chem. 9: 1629-1644.

20 Graef M, McHenry ME Structure of materials. An introduction to crystallography, diffraction and symmetry; Second Ed.; Cambridge University Press: Cambridge, 2012; ISBN 978-1-107-00587-7.)

21. Mäntymäki M, Ritala M, Leskelä M, (2012) Coord. Chem. Rev. 256:854-877.

22. Kuhlman R, Vaartstra BA, Streib WE, Huffman JC, Caulton KG (1993) Inorg. Chem. 32:1272-1278.

23. Mehrotra RC, Singh A, Sogani S (1994) Chem. Rev. 94:1643-1660.

24. Colomban P, Zaafrani O, Slodczyk A (2012) Membranes (Basel) 2: 493-509.

25. Slodczyk A, Tran C, Colomban P (2012)MRS Proc. 1309:mrsf10-1309-ee03-21:1–mrsf10-1309-ee03-21:6..

26. Rose BA, Davis GJ, Ellingham HJT (1948) Discuss. Faraday Soc. 4:154-162.

27. Slodczyk A, Colomban P, Willemin S, Lacroix O, Sala B (2009) J. Raman Spectrosc. 40: 513-521.

28. Slodczyk A, Colomban P (2010) Materials (Basel). 3: 5007-5028.

29. Slodczyk A, Limage MH, Colomban P, Zaafrani O, Grasset F, Loricourt J, Sala B, J. Raman Spectrosc. 42 (2011) 2089-2099:.

30. Gouadec G, Colomban P (2007) Prog. Cryst. Growth Charact. Mater. 53: 1-56.

31. Slodczyk A, Colomban P, Upasen S, Grasset F, André G (2015) J. Phys. Chem. Solids 83:85-95.

32. Athar T (2013) Mater. Focus 2:450-453.

33. Siebert E, Boréave A, Gaillard F, Pagnier T, Solid State Ionics (2013) 247–248:30-40.

34. Pérez-Coll D, Céspedes E, Dos santos-García AJ, Mather GC, Prieto C (2014) J. Mater. Chem. A2: 7170-7174-.

35. Pérez-Coll D, Heras-Juaristi G, Fagg DP, Mather GC (2014) J. Power Sources 245:445-455.

36. Nowick A, Vaysleyb A (1997) Solid State Ionics 97:17-26.

Figure captions

Fig. 1 Scanning electron micrographs of the $SrZr_{0.9}Y_{0.1}O_{3-\delta}$ sol-gel coating surface heat treated at **a** 700 ºC for 1 hour, **b** 800 ºC for 1 hour (energy dispersive X-ray spectroscopy (EDX) plots for the coating surface are shown as insets) and **c** scanning electron micrograph of a cross-section of the $SrZr_{0.9}Y_{0.1}O_{3-\delta}$ sol-gel coating heat treated at 700 ºC for 1 hour.

Fig. 2 X-ray diffraction patterns of sol-gel coatings heat-treated at different temperatures for one hour.

Fig. 3 a Transmission electron micrograph of $SrZr_{0.9}Y_{0.1}O_{3-\delta}$ sol-gel coating treated at 800 ºC for 1 hour, and **b** magnified image revealing the [002] lattice plane of the orthorhombic SZY phase (JCPS 44-0161).

Fig. 4 Micro-Raman spectra of the sol-gel coatings treated at 700, 800 and 900 °C for one hour in the range 1000–100 cm^{-1}.

Fig. 5 Impedance spectroscopy plots of SZY film deposited on quartz substrate collected at 700 °C in H_2O- and D_2O-wetted air; numbers refer to $\log_{10}$ of the frequency.

Fig. 6 Arrhenius representation of the electrical conductivity in wet air of the SZY thin film compared to the results of SZY prepared as cylindrical pellets [7]. SZY1600 corresponds to a pellet sintered at 1600 ºC and SZYZn1300 to a pellet prepared after the addition of 4 mol % ZnO and sintered at 1300 ºC.

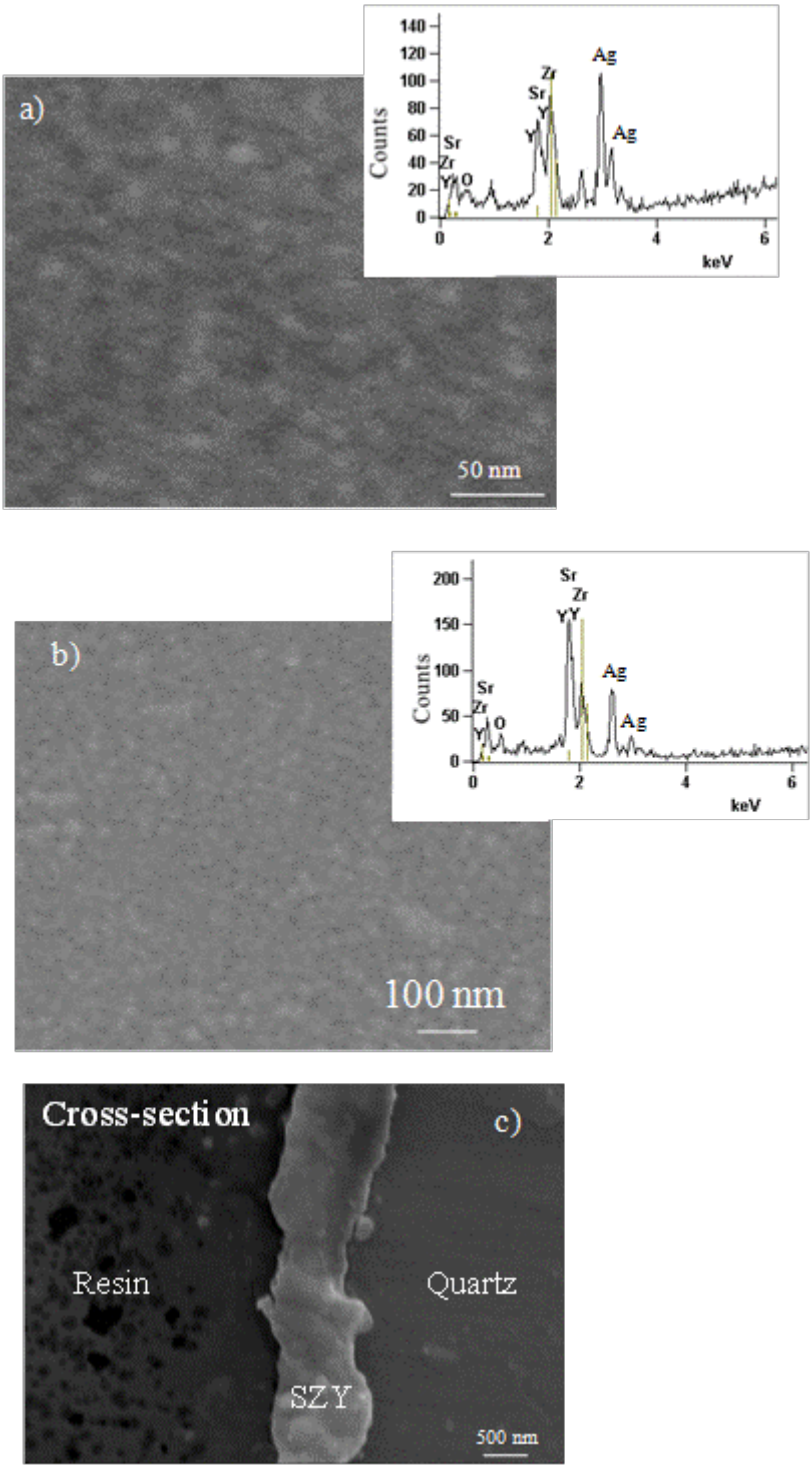

Fig. 1 Scanning electron micrographs of the $SrZr_{0.9}Y_{0.1}O_{3-\delta}$ sol-gel coating surface heat treated at **a** 700 ºC for 1 hour, **b** 800 ºC for 1 hour (energy dispersive X-ray spectroscopy (EDX) plots for the coating surface are shown as insets) and **c** scanning electron micrograph of a cross-section of the $SrZr_{0.9}Y_{0.1}O_{3-\delta}$ sol-gel coating heat treated at 700 ºC for 1 hour.

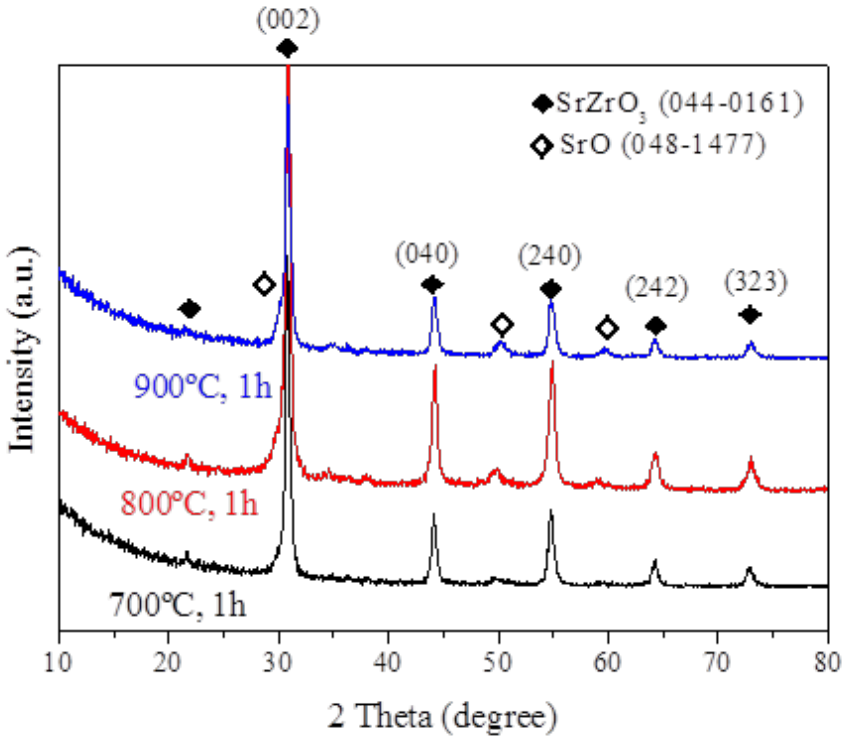

Fig. 2 X-ray diffraction patterns of sol-gel coatings heat-treated at different temperatures for one hour.

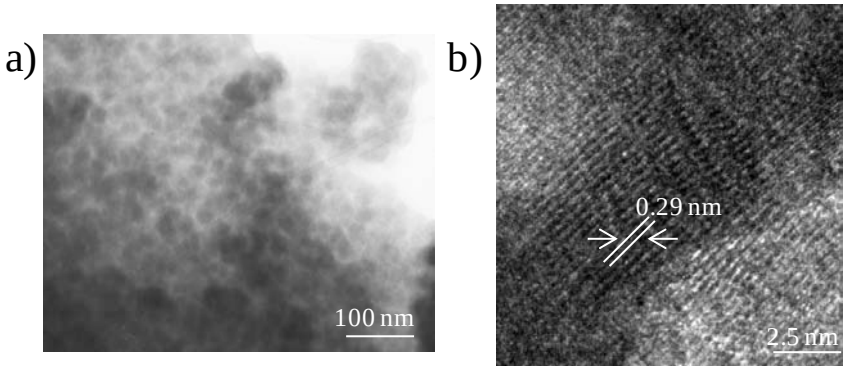

Fig. 3 a Transmission electron micrograph of $SrZr_{0.9}Y_{0.1}O_{3-\delta}$ sol-gel coating treated at 800 ºC for 1 hour, and **b** magnified image revealing the [002] lattice plane of the orthorhombic SZY phase (JCPS 44-0161).

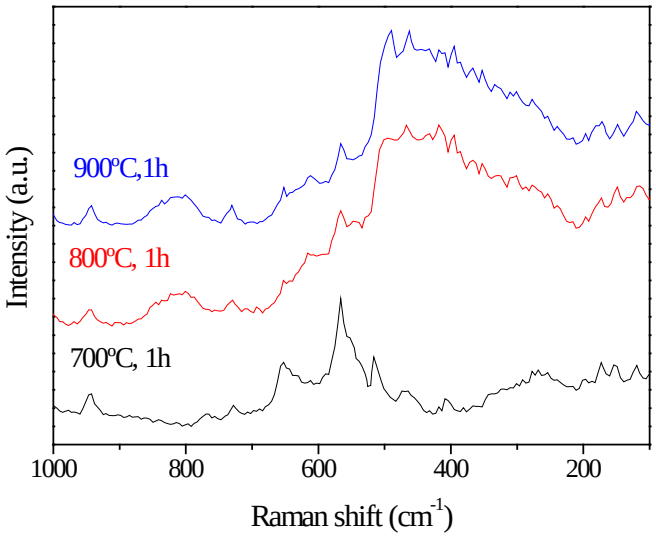

Fig. 4 Micro-Raman spectra of the sol-gel coatings treated at 700, 800 and 900 °C for one hour in the range 1000–100 cm^{-1}.

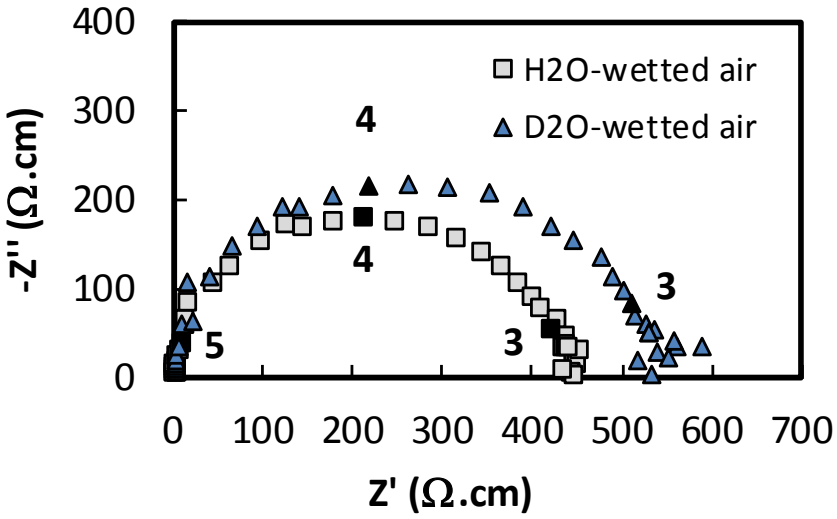

Fig. 5 Impedance spectroscopy plots of SZY film deposited on quartz substrate collected at 700 °C in H_2O- and D_2O-wetted air; numbers refer to $\log_{10}$ of the frequency.

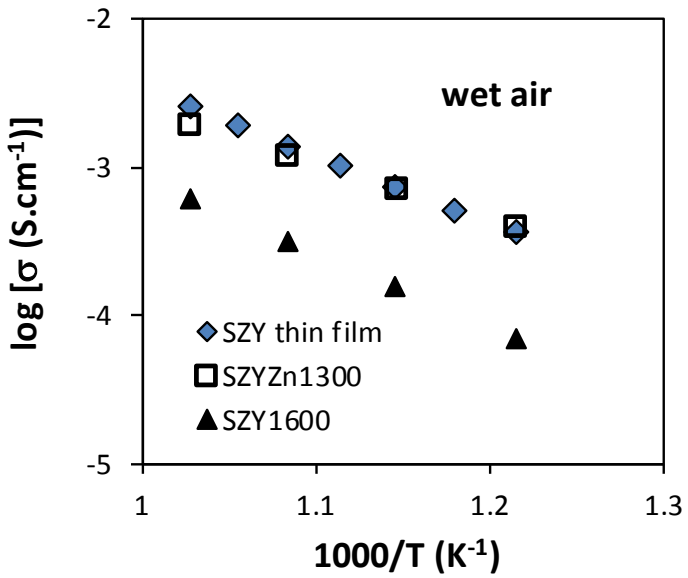

Fig. 6 Arrhenius representation of the electrical conductivity in wet air of the SZY thin film compared to the results of SZY prepared as cylindrical pellets [7]. SZY1600 corresponds to a pellet sintered at 1600 ºC and SZYZn1300 to a pellet prepared after the addition of 4 mol % ZnO and sintered at 1300 ºC.